

Effect of Tm^{3+} -induced defects on the photoexcitation energy relaxation in Tm-doped $\text{Al}_x\text{Ga}_{1-x}\text{N}$

Y. D. Glinka*

Institute of Physics, National Academy of Sciences of Ukraine, Kiev 03028, Ukraine

H. O. Everitt

*U.S. Army Aviation and Missile RDEC, Redstone Arsenal, Huntsville, Alabama 35809, USA
and Department of Physics, Duke University, Durham, North Carolina 27708, USA*

D. S. Lee and A. J. Steckl

Nanoelectronics Laboratory, University of Cincinnati, Cincinnati, Ohio 45221, USA

(Received 22 January 2009; published 27 March 2009)

We provide evidence that the Tm^{3+} -induced defects in Tm-doped $\text{Al}_x\text{Ga}_{1-x}\text{N}$ hosts play a major role in the nonradiative transfer of the excitation energy from the 1I_6 state to the 1D_2 state of Tm^{3+} ions from which the most efficient photoluminescence (PL) transition (465 nm) occurs. Once the concentration of the Tm^{3+} -induced defects decreases with increasing x , the PL transitions starting from the 1I_6 state (298, 357, 395, 530, and 785 nm) may be significantly enhanced. It is shown that the indirect excitation of the 1I_6 state results from the Auger-type energy transfer due to the nonradiative band-to-band recombinations in the $\text{Al}_x\text{Ga}_{1-x}\text{N}$ host of a given x . In contrast, the PL transitions starting from the 1G_4 level (479 and 807 nm) can be excited through either an indirect or a direct regime. In both cases the 1G_4 level is populated by the radiative relaxation of the higher energy excited states 1I_6 , 3P_0 , 3P_1 , and 3P_2 of Tm^{3+} ions.

DOI: [10.1103/PhysRevB.79.113202](https://doi.org/10.1103/PhysRevB.79.113202)

PACS number(s): 78.55.-m, 71.55.Eq, 76.30.Kg

Rare-earth (RE) ions implanted into semiconductors present an interesting possibility for the integrated light-emitting devices in the ultraviolet (UV) range.¹⁻³ Despite the numerous known applications of RE-doped III-V semiconductors for linear and nonlinear optics and laser physics, the detailed picture of the energy transfer from the semiconductor host to RE ions has remained unclear. Up to now it is known that the carriers excited in the $\text{Al}_x\text{Ga}_{1-x}\text{N}$ materials dramatically increase the effective excitation cross section of RE ions resulting in the excitation of their intra-4f electron transitions followed by efficient light emission.¹⁻³ As a mechanism of RE-related photoluminescence (PL) excitation the Auger-type process has been proposed, which involves the nonradiative energy transfer to RE ions released from the band-to-band recombinations in the $\text{Al}_x\text{Ga}_{1-x}\text{N}$ host.¹

However, the Auger-type model has to be clarified in more detail especially with reference to the recent local density functional calculation of RE dopants in GaN and AlN, which point to the RE-induced defects in the vicinity of RE ions.⁴⁻⁶ In the current Brief Report we present the results of the study of PL and photoluminescence excitation (PLE) on the Tm-doped $\text{Al}_x\text{Ga}_{1-x}\text{N}$ materials of different Al content (x). We show that the PLE spectra vary significantly with x as a consequence of the variation in the band-gap energy of $\text{Al}_x\text{Ga}_{1-x}\text{N}$ materials. As a result, both the direct and indirect regimes of the excitation of Tm^{3+} -related PL from the Tm-doped $\text{Al}_x\text{Ga}_{1-x}\text{N}$ materials have been experimentally observed. The direct excitation of Tm^{3+} ions occurs mainly for PL transitions starting from the 1G_4 level, which is populated due to the radiative relaxation of the higher energy excited states 1I_6 , 3P_0 , 3P_1 , and 3P_2 if they do not overlap with the conduction-band states of the $\text{Al}_x\text{Ga}_{1-x}\text{N}$ materials of a given x . The indirect mechanism can be realized through the excitation of free carriers in the $\text{Al}_x\text{Ga}_{1-x}\text{N}$ hosts followed by the Auger-type nonradiative energy transfer to Tm^{3+} ions. We found that the Tm^{3+} -induced defect plays a major role in the

nonradiative transfer of the excitation energy from the 1I_6 state to the 1D_2 state of Tm^{3+} from which the most efficient PL transition occurs (465 nm). Also we stated that the Tm^{3+} -induced defects are predominantly formed in the $\text{Al}_x\text{Ga}_{1-x}\text{N}$ materials of a small x . The energy transfer to 1D_2 state hence decreases with increasing x leading to transitions from the 1I_6 state to be enhanced and giving rise to intense UV PL peaked at 298 nm.

Tm-doped $\text{Al}_x\text{Ga}_{1-x}\text{N}$ materials of $x=0.39, 0.62, 0.81,$ and 1.0 used in the current study were grown by solid-source molecular-beam epitaxy on p -type Si (111) substrates. The peculiarities of the growth procedure have been previously discussed.⁷ The tunable light source for PLE spectroscopy was a xenon arc lamp dispersed through an Acton 150 mm monochromator. The PL was analyzed by a 0.75 m focal length Spex single grating monochromator and detected by a thermoelectrically cooled photomultiplier tube (Hamamatsu R928). Standard lock-in technique was used for collecting both PL and PLE signals. All PL and PLE spectra were corrected for the spectral sensitivity of the apparatus and changes in the excitation power of a xenon arc lamp with wavelength, respectively. An optical parametric amplifier (OPA) pumped by a 1 kHz regenerative amplifier seeded by an 80 MHz Ti:Sa oscillator operating at 790 nm in combination with the Topas light conversion system has been used as a pulsed source for time-integrated and time-resolved PL measurements. In our experiments the 238 nm (5.21 eV) light of an average intensity of 20 mW and pulse width ~ 200 fs has been used to excite PL. The PL response has been monitored either by a charge-coupled device camera or by a streak camera through the fiber optics and monochromators. The streak camera temporal resolution edge was 30 ps.

Figure 1 shows the PL spectra for Tm-doped $\text{Al}_x\text{Ga}_{1-x}\text{N}$ materials of different x measured at 85 K. The spectra reveal several sharp features, which have normally been observed

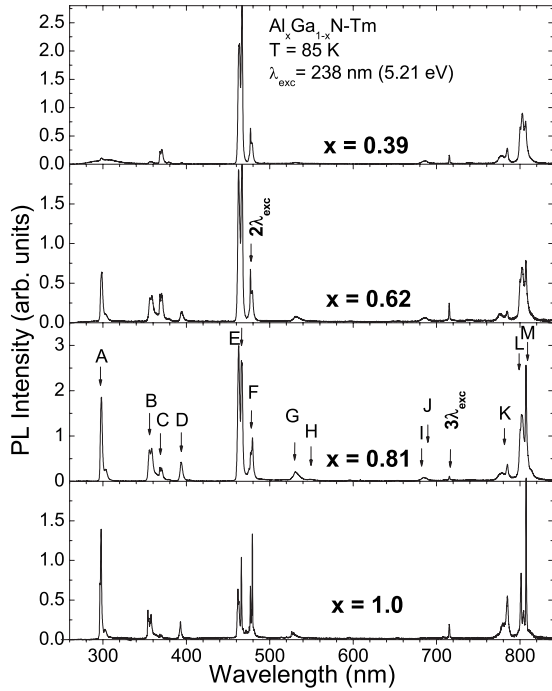


FIG. 1. PL spectra for $\text{Al}_x\text{Ga}_{1-x}\text{N-Tm}^{3+}$ of different x measured with 238 nm (5.21 eV) excitation at 85 K. The PL peaks assigned to transitions between the corresponding multiplet manifolds are indicated by arrows and labeled by caps in accordance with transitions shown in Fig. 2. $2\lambda_{\text{exc}}$ and $3\lambda_{\text{exc}}$ denote the second and third orders of the grating scattering of the excitation laser light, respectively.

in a variety of wide band-gap Tm-doped materials and attributed to intra-4f electron transitions in Tm^{3+} ions (Fig. 1).^{2,8} Also, because of the crystal-field splitting effect, each of the peaks shows an additional fine structure.⁸ The Tm^{3+} ion energy diagram for the $\text{Al}_x\text{Ga}_{1-x}\text{N-Tm}^{3+}$ materials of different x and transitions between multiplet manifolds normally observed is shown in Fig. 2. Correspondingly, the dominating blue emission at around 465 nm is attributed to the 1D_2

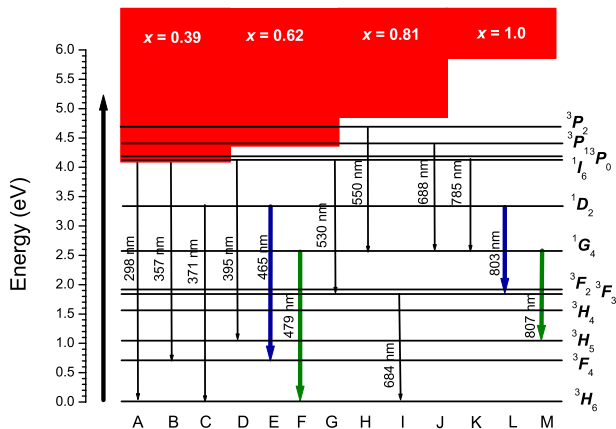


FIG. 2. (Color online) Tm^{3+} energy diagram for $\text{Al}_x\text{Ga}_{1-x}\text{N-Tm}^{3+}$ and the corresponding transitions between multiplet manifolds (shown on the right) which were observed in PL spectra (the caps below mark transitions shown in Fig. 1). The conduction-band states for the $\text{Al}_x\text{Ga}_{1-x}\text{N}$ materials of different x are shown in red. The photon energy of the excitation laser light used is indicated by an arrow on the left.

$\rightarrow ^3F_4$ electron transition in Tm^{3+} ion. Less intense peaks have been assigned to transitions starting from the 3P_1 , 3P_2 , 1I_6 , 1D_2 , 1G_4 , and 3F_3 multiplet manifolds (Fig. 2).^{2,8} The excitation energy used (5.21 eV) is that best suited to excite the free carriers in all the $\text{Al}_x\text{Ga}_{1-x}\text{N}$ materials of $x=0.39$, 0.62, and 0.81, except that of $x=1.0$ (Fig. 2). The excitation of Tm^{3+} ions hence is indirect for the $\text{Al}_x\text{Ga}_{1-x}\text{N-Tm}^{3+}$ materials of $x=0.39$, 0.62, and 0.81, while for that of $x=1$ the direct excitation of Tm^{3+} ions through their higher energy excited states can exclusively be realized. The most intense PL is observed for the $\text{Al}_x\text{Ga}_{1-x}\text{N-Tm}^{3+}$ materials of $x=0.81$ for which the photon energy is slightly in excess of the band-gap energy (Figs. 1 and 2). Alternatively, for the $\text{Al}_x\text{Ga}_{1-x}\text{N-Tm}^{3+}$ materials of $x=0.39$ and 0.62 the PL intensity slightly decreases as a consequence of the less efficient energy transfer to Tm^{3+} ions governed by energetic (hot) carriers. We associate this peculiarity with a decrease in the trapping rate for hot carriers. If the 5.21 eV excitation is applied to the $\text{Al}_x\text{Ga}_{1-x}\text{N-Tm}^{3+}$ materials of $x=1.0$, the PL intensity is reduced because of the direct excitation regime.

Additionally to the sharp features discussed, a broad PL band peaked at around 300 nm is also observed for the $\text{Al}_x\text{Ga}_{1-x}\text{N}$ host of $x=0.39$, which can be associated with the band-to-band PL from the $\text{Al}_x\text{Ga}_{1-x}\text{N}$ host (Fig. 1). The band-to-band PL from the $\text{Al}_x\text{Ga}_{1-x}\text{N}$ materials of larger x is believed to occur beyond the spectral range accessible. The existence of the band-to-band PL is a strong support for the Auger-type mechanism of indirect PL excitation in Tm-doped $\text{Al}_x\text{Ga}_{1-x}\text{N}$ to be applied. The energy of the band-to-band recombinations in the $\text{Al}_x\text{Ga}_{1-x}\text{N}$ host hence can be transferred nonradiatively to one of the higher energy excited states 3P_0 , 3P_1 , 3P_2 , and 1I_6 in Tm^{3+} ions depending on the band-gap energy of the $\text{Al}_x\text{Ga}_{1-x}\text{N}$ host of a given x .

The lifetime of Tm^{3+} -related light emitters has been measured for most intense peaks in the time-resolved mode. The decay of PL reveals a single exponential behavior. The corresponding decay-time constants measured at 85 K for different PL peaks mentioned are the following: 1.5 (A), 1.5 (B), 1.7 (C), 1.5 (D), 1.1 (E), and 14.7 μs (F). The band-to-band PL is characterized by a short-time decay, which is shorter than the temporal resolution edge of the streak camera used (30 ps). This is consistent with the time-resolved measurements of the $\text{Al}_x\text{Ga}_{1-x}\text{N}$ materials.⁹ The Tm^{3+} -related PL decays slowly, which is in agreement with that observed previously.² The decay-time constants obtained are unaffected by Al content in the $\text{Al}_x\text{Ga}_{1-x}\text{N}$ materials. This suggests that the temporal dynamics is completely determined by the final stage of the energy relaxation (radiative) and all the processes of energy transfer between the hosts and Tm^{3+} ions occur in the time frame which is much shorter than the lifetime of light emitters.

The position of most intense PL peaks marked in Fig. 1 has been used as a registration wavelength (λ_{reg}) to measure the corresponding PLE spectra. As we might expect, the PL from Tm^{3+} ions is mostly excited indirectly through the excitation of free carriers in the $\text{Al}_x\text{Ga}_{1-x}\text{N}$ hosts. This is exemplified in Fig. 3 for the $\text{Al}_x\text{Ga}_{1-x}\text{N}$ host of $x=0.81$. As a result, the PL intensity for the majority of peaks rises up by following the fundamental absorption edge of the $\text{Al}_x\text{Ga}_{1-x}\text{N}$ material. There is only one exception from the mentioned

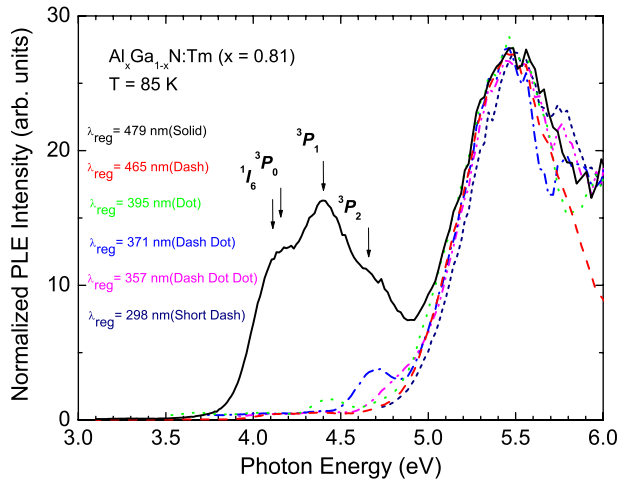


FIG. 3. (Color online) PLE spectra at 85 K for $\text{Al}_x\text{Ga}_{1-x}\text{N-Tm}^{3+}$ of $x=0.81$. Spectra measured at different λ_{reg} are shown by the corresponding colors/grayscale. The higher energy excited states of Tm^{3+} are indicated by arrows.

general rule, which deals with the peak at around 479 nm assigned to the $^1G_4 \rightarrow ^3H_6$ transition. In the latter case the PL can be excited either indirectly through the excitation of free carriers in the $\text{Al}_x\text{Ga}_{1-x}\text{N}$ host or directly through the excitation of the higher energy excited states of Tm^{3+} ions (shown by arrows in Fig. 3). One can see that even if the direct excitation regime can be realized for other PL peaks, its efficiency is at least tenfold less than that for the 479 nm peak. The mentioned peculiarity of the PL peak at around 479 nm is also appeared for the $\text{Al}_x\text{Ga}_{1-x}\text{N}$ hosts with $x=0.39, 0.62,$ and 1.0 indicating that the principally different pathway of the excitation energy relaxation appeared through the 479 nm PL peak as compared to the rest of the peaks. To analyze that we select PLE spectra measured only within two PL features peaked at around 465 ($^1D_2 \rightarrow ^3F_4$ transition) and 479 nm ($^1G_4 \rightarrow ^3H_6$ transition) (Fig. 4). The PLE spectra measured with $\lambda_{\text{reg}}=465$ nm reveal the pronounced shift of the absorption edge position for the $\text{Al}_x\text{Ga}_{1-x}\text{N}$ materials toward the higher energy range as x increases from $x=0.39$ to $x=1.0$. There is nothing surprising that the fundamental absorption edge slightly shifts (~ 35 meV) toward the higher energy range for all the materials studied with decreasing temperature from 300 to 85 K. This is consistent with Varshni's equation.¹⁰

The band-gap energies estimated from PLE spectra taken at 85 K are 4.07 ($x=0.39$), 4.36 ($x=0.62$), 4.85 ($x=0.81$), and 5.82 eV ($x=1.0$). The latter value is slightly less than that known for AlN (6.12 eV) (Ref. 5) because of the limit of the setup sensitivity in the UV range. Also, one can see a very weak contribution peaked at around 3.35 eV which is due to the direct excitation through the $^3H_6 \rightarrow ^1D_2$ transition. Because the PLE spectra measured with $\lambda_{\text{reg}}=479$ nm consist of two contributions (direct and indirect excitations) while the PLE spectra measured with $\lambda_{\text{reg}}=465$ nm mainly show an indirect excitation regime, one can analyze the difference between the PLE spectra measured with $\lambda_{\text{reg}}=479$ nm and $\lambda_{\text{reg}}=465$ nm in order to get only directly excited part of PL from Tm^{3+} ions [Fig. 4(b)].

The resulting PLE spectra in general show three contribu-

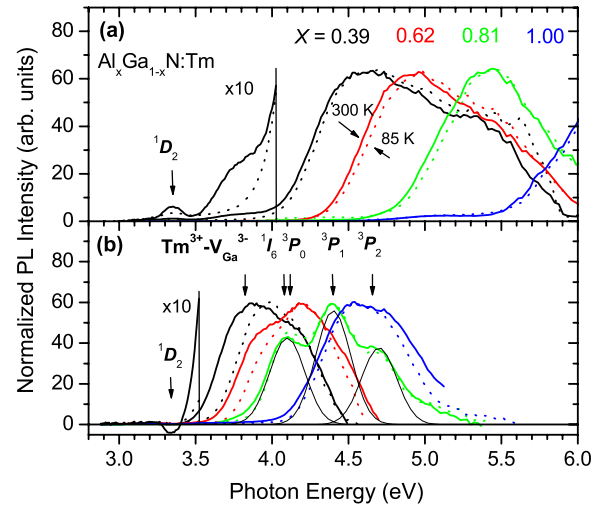


FIG. 4. (Color online) (a) PLE spectra at 300 (solid lines) and 85 K (dot lines) measured with $\lambda_{\text{reg}}=465$ nm for $\text{Al}_x\text{Ga}_{1-x}\text{N-Tm}^{3+}$ of different x indicated by the corresponding colors (the corresponding curves shift toward the higher energy range with increasing x). (b) Difference of PLE spectra measured with $\lambda_{\text{reg}}=479$ and 465 nm at the same temperatures [colors/different grayscale correspond to those shown in (a)]. Tm^{3+} excited states and $\text{Tm}^{3+}-V_{\text{Ga}}^{3-}$ complex state are indicated by arrows. The part of the PLE spectra for $\text{Al}_x\text{Ga}_{1-x}\text{N-Tm}^{3+}$ of $x=0.39$ is also shown on the tenfold enlarged scale. The negative feature that appeared at around 3.35 eV in (b) is a result of the subtraction of the PL intensity excited through the $^3H_6 \rightarrow ^1D_2$ transition appeared in (a). Gaussian profiles of $^3H_6 \rightarrow ^1I_6$, ($^3H_6 \rightarrow ^3P_0$), $^3H_6 \rightarrow ^3P_1$, and $^3H_6 \rightarrow ^3P_2$ transitions are exemplified in the PLE spectrum for $\text{Al}_x\text{Ga}_{1-x}\text{N-Tm}^{3+}$ with $x=0.81$ by thin black lines.

tions which cover the spectral range originated from the transitions $^3H_6 \rightarrow ^1I_6$, $^3H_6 \rightarrow ^3P_0$, $^3H_6 \rightarrow ^3P_1$, and $^3H_6 \rightarrow ^3P_2$ in Tm^{3+} ions (Fig. 2). Specifically, the spectra extend toward the higher energy range with increasing x because of the rise in the band-gap energy and so the more that energetic transitions in Tm^{3+} ions contribute to the PLE spectra with increasing x since they do not overlap with the conduction-band states of the $\text{Al}_x\text{Ga}_{1-x}\text{N}$ materials of a given x (Figs. 2 and 4). Correspondingly, the $\text{Al}_x\text{Ga}_{1-x}\text{N}$ host of $x=0.81$ reveals all three contributions mentioned which can be fitted by Gaussian profiles [Fig. 4(b)]. However, there is some excitation of PL below the mentioned spectral range, which fills up the energy gap between the 1I_6 and 1D_2 levels (the energy range of 3.35–4.1 eV). This is mainly observed for the $\text{Al}_x\text{Ga}_{1-x}\text{N}$ hosts with $x=0.39$ and 0.62 [Fig. 4(b)]. It should be particularly emphasized that the range under discussion lies below the absorption edges for any $\text{Al}_x\text{Ga}_{1-x}\text{N}$ materials studied (Fig. 2). This suggests that there exists an additional absorption band, which is energetically positioned between the 1I_6 and 1D_2 levels of Tm^{3+} ions. We associate this absorption band with Tm^{3+} -induced defects. The position of the band, which is peaked at around of 3.8 eV, is consistent with the energy required for capture of an electron excited from the valence band by the neutral $\text{Tm}^{3+}-V_{\text{Ga}}^{3-}$ complex, where V_{Ga}^{3-} is a nitrogen vacancy.⁵ The mentioned absorption band is expected to be a key circumstance for the excitation energy relaxation between the 1I_6 and 1D_2 levels. The energetic dis-

tance between these levels is larger than 750 meV, which can only be bridged in the nonradiative energy relaxation process by more than seven longitudinal optical (LO) phonons in the $\text{Al}_x\text{Ga}_{1-x}\text{N}$ hosts, a process which is rather unlikely.¹¹ The existence of the defect-related states removes this restriction, giving rise to intense PL associated with transitions starting from the 1D_2 level. We extend hence the defect-mediated energy transfer mechanism to the Tm-doped $\text{Al}_x\text{Ga}_{1-x}\text{N}$ materials, which has earlier been discussed for InP:Yb and Si:Er systems.^{12,13} Since the mentioned nonradiative transfer of the excitation energy is highly efficient and since the 1I_6 state in Tm^{3+} ions is excited through the Auger-type process, the PLE spectra for PL transitions starting from the 1I_6 and 1D_2 levels follow the fundamental absorption edge of the $\text{Al}_x\text{Ga}_{1-x}\text{N}$ materials of a given x . As this takes place, further nonradiative energy relaxation from the 1D_2 level to the 1G_4 level is less probable since it can only be realized through the multiplied LO-phonon emission mentioned above.

The existence of the additional absorption band associated with Tm^{3+} -induced defects is also supported by the temperature dependence of the PLE spectra (Fig. 4). As we mentioned above, the part of the PLE spectra originated from the band-to-band transitions [Fig. 4(a)] just slightly blueshifts with decreasing temperature from 300 to 85 K. The part of the PLE spectra related to the Tm^{3+} ion higher energy excited states [Fig. 4(b)] remains almost unchanged with decreasing temperature. Alternatively, the temperature effect on the additional absorption band associated with Tm^{3+} -induced defects is unusually big. The blueshift observed for $\text{Al}_x\text{Ga}_{1-x}\text{N}$ hosts with $x=0.39$ and 0.62 is estimated to be ~ 120 meV. Such a dynamics of PLE spectra with temperature requires additional theoretical consideration and will be discussed elsewhere. Another very important finding is that the Tm^{3+} -induced defects are predominantly formed in the $\text{Al}_x\text{Ga}_{1-x}\text{N}$ materials of a small x . As a result, the nonradiative energy transfer from the 1I_6 state to the 1D_2 state of Tm^{3+} decreases with increasing x , leading to transitions from the 1I_6 state to be enhanced and giving rise to intense PL peaked at 298, 357, 396, 530, and 785 nm.

Now we turn to the directly excited PL which appears mainly through the 479 nm PL peak. Here we state that the energy of excitation from the 1I_6 , 3P_0 , 3P_1 , and 3P_2 excited states can be transferred to the 1G_4 level radiatively by emitting 785 ($^1I_6(^3P_0) \rightarrow ^1G_4$ transition), 688 ($^3P_1 \rightarrow ^1G_4$ transi-

tion), and 550 nm light ($^3P_2 \rightarrow ^1G_4$ transition) (Fig. 2). Thus, the energy of the 1I_6 (3P_0), 3P_1 , and 3P_2 excited states initially transfers to the 1G_4 level radiatively and then effectively relaxes to the 3H_6 and 3H_5 levels also by the radiative transitions. The resulting 479 and 807 nm PL peaks hence get stronger with increasing x as compared to the 465 nm peak because the efficiency of the energy relaxation pathway through the 1D_2 state decreases as we mentioned above. This is also a reason why the PLE spectra measured with $\lambda_{\text{reg}} = 479$ nm ($^1G_4 \rightarrow ^3H_6$ transition) reveal the highly efficient direct excitation of Tm^{3+} ions in $\text{Al}_x\text{Ga}_{1-x}\text{N}$ hosts. Here we note again that the nonradiative relaxation of the higher energy excited 3P_1 and 3P_2 states to the 1I_6 state is less probable since it requires the multiplied LO-phonon emission process to be realized.¹¹ Also, one can see that the radiative relaxation through the $^1I_6(^3P_0) \rightarrow ^1G_4$ transition decreases with increasing x [Fig. 4(b)]. This is consistent with the fact mentioned above that other radiative transitions from the 1I_6 state are enhanced by increasing x .

In summary, we have provided evidence that the Tm^{3+} -induced defects in Tm-doped $\text{Al}_x\text{Ga}_{1-x}\text{N}$ hosts play a major role in the nonradiative transfer of the excitation energy to the Tm^{3+} state from which the most efficient PL transition occurs. The direct and indirect excitation regimes of PL from Tm-doped $\text{Al}_x\text{Ga}_{1-x}\text{N}$ materials of different Al content have been recognized. The indirect excitation occurs through the Auger-type nonradiative process at which the higher energy excited states 1I_6 , 3P_0 , 3P_1 , and 3P_2 of Tm^{3+} ions may be excited depending on the band-gap energy of the $\text{Al}_x\text{Ga}_{1-x}\text{N}$ hosts of a given x . Further nonradiative energy relaxation from the 1I_6 state to the 1D_2 state involves the Tm^{3+} -induced defects. Finally, the most intense PL transitions from the 1D_2 state occur (465 nm). The direct excitation regime is shown to be efficient enough only for PL transitions starting from the 1G_4 level (479 and 807 nm), which is populated by the radiative relaxation of the higher energy excited states 1I_6 , 3P_0 , 3P_1 , and 3P_2 of Tm^{3+} ions if they do not overlap with the conduction-band states of the $\text{Al}_x\text{Ga}_{1-x}\text{N}$ host of a given x .

One of the authors (Y.D.G.) gratefully acknowledges support from the U. S. Army Aviation and Missile RDEC. The work at Cincinnati was supported in part by the U. S. Army Research Office (Contract No. DAAD19-03-1-0101).

*On leave from U. S. Army Aviation and Missile RDEC, Redstone Arsenal, Alabama 35809, USA; yuridlinka@yahoo.com

¹S. Schmitt-Rink, C. M. Varma, and A. F. J. Levi, Phys. Rev. Lett. **66**, 2782 (1991).

²U. Hommerich, E. E. Nyein, D. S. Lee, A. J. Steckl, and J. M. Zavada, Appl. Phys. Lett. **83**, 4556 (2003).

³H. Peng, C.-W. Lee, H. O. Everitt, C. Munasinghe, D. C. Lee, and A. J. Steckl, J. Appl. Phys. **102**, 073520 (2007).

⁴J. Neugebauer and C. G. Van de Walle, Appl. Phys. Lett. **69**, 503 (1996).

⁵S. Petit, R. Jones, M. J. Shaw, P. R. Briddon, B. Hourahine, and T. Frauenheim, Phys. Rev. B **72**, 073205 (2005).

⁶J.-S. Filhol, R. Jones, M. J. Shaw, and P. R. Briddon, Appl. Phys. Lett. **84**, 2841 (2004).

⁷D. S. Lee and A. J. Steckl, Appl. Phys. Lett. **83**, 2094 (2003).

⁸J. B. Gruber, U. Vetter, H. Hofsass, B. Zandi, and M. F. Reid, Phys. Rev. B **70**, 245108 (2004).

⁹U. Özgür, H. O. Everitt, L. He, and H. Morkoc, Appl. Phys. Lett. **82**, 4080 (2003).

¹⁰J. Wu, W. Walukiewicz, W. Shan, K. M. Yu, J. W. Ager, S. X. Li, E. E. Haller, H. Lu, and W. J. Schaff, J. Appl. Phys. **94**, 4457 (2003).

¹¹L. Riseberg and H. Moos, Phys. Rev. **174**, 429 (1968).

¹²M. A. J. Klik, T. Gregorkiewicz, I. V. Bradley, and J.-P. R. Wells, Phys. Rev. Lett. **89**, 227401 (2002).

¹³I. Tsimperidis, T. Gregorkiewicz, H. H. P. Th. Bekman, and C. J. G. M. Langerak, Phys. Rev. Lett. **81**, 4748 (1998).